STEM CELLS TRANSLATIONAL MEDICINE®

ENABLING TECHNOLOGIES FOR CELL-BASED CLINICAL TRANSLATION

Enabling Large-Scale Ex Vivo Production of Megakaryocytes from CD34$^+$ Cells Using Gas-Permeable Surfaces

ANDRES F. MARTINEZ,[a] WILLIAM M. MILLER [a,b]

Key Words. Megakaryocyte • CD34$^+$ • Thrombopoiesis • Cell culture • Cellular therapy

[a]Department of Chemical and Biological Engineering, Northwestern University, Evanston, Illinois, USA; [b]Robert H. Lurie Comprehensive Cancer Center, Northwestern University, Evanston, Illinois, USA

Correspondence: William M. Miller, Ph.D., Northwestern University, Department of Chemical and Biological Engineering, 2145 Sheridan Rd., Tech E136, Evanston, Illinois 60208-3120, USA. Telephone: 847-491-4828; e-mail: wmmiller@northwestern.edu

Received July 22, 2018; accepted for publication February 6, 2019; first published March 8, 2019.

http://dx.doi.org/10.1002/sctm.18-0160

ABSTRACT

Patients suffering from acute or sustained thrombocytopenia require platelet transfusions, which are entirely donor-based and limited by challenges related to storage and fluctuating supply. Developing cell-culture technologies will enable ex vivo and donor-independent platelet production. However, critical advancements are needed to improve scalability and increase megakaryocyte (Mk) culture productivity. To address these needs, we evaluated Mk production from mobilized peripheral blood CD34$^+$ cells cultured on a commercially available gas-permeable silicone rubber membrane, which provides efficient gas exchange, and investigated the use of fed-batch media dilution schemes. Starting with a cell-surface density of 40×10^3 CD34$^+$ cells per cm^2 (G40D), culturing cells on the membrane for the first 5 days and employing media dilutions yielded 39 $\pm$ 19 CD41$^+$CD42b$^+$ Mks per input CD34$^+$ cell by day 11—a 2.2-fold increase compared with using standard culture surfaces and full media exchanges. By day 7, G40D conditions generated 1.5-fold more CD34$^+$ cells and nearly doubled the numbers of Mk progenitors. The increased number of Mk progenitors coupled with media dilutions, potentially due to the retention of interleukin (IL)-3, increased Mk production in G40D. Compared with controls, G40D had higher viability, yielded threefold more Mks per milliliter of media used and exhibited lower mean ploidy, but had higher numbers of high-ploidy Mks. Finally, G40D-Mks produced proplatelets and platelet-like-particles that activate and aggregate upon stimulation. These results highlight distinct improvements in Mk cell-culture and demonstrate how new technologies and techniques are needed to enable clinically relevant production of Mks for platelet generation and cell-based therapies. STEM CELLS TRANSLATIONAL MEDICINE *2019;8:658–670*

SIGNIFICANCE STATEMENT

Patients suffering from thrombocytopenia require platelet transfusions, which are entirely donor-based. Donor platelets are limited by a 5-day shelf life, fluctuating supply, risk of contamination, and alloimmunization. Developing cell-culture technologies for megakaryocytes (Mks) from blood stem and progenitor (CD34$^+$) cells would enable ex vivo and donor-independent platelet production. In the present study, a gas-permeable culture surface alongside fed-batch media dilution schemes for the production of Mks from CD34$^+$ cells was evaluated. Increasing the seeding cell-surface density on the gas-permeable surface led to increased expansion of Mk progenitors and, when coupled with fed-batch media dilution schemes, enhanced Mk production compared with standard tissue culture surfaces with full media exchanges. These results demonstrate the need to develop cell-culture technologies to enable clinically relevant production of Mks for platelet generation and cell-based therapies.

INTRODUCTION

Close to 2 million platelets units are transfused annually in the U.S. to treat patients with defective platelets or low blood platelet counts [1, 2]. Currently, platelet transfusions are entirely dependent on human volunteer donors, and these methods are limited by a 5-day shelf life, risk of contamination, and differences in donor/recipient immunology [1]. There is great interest in generating platelets ex vivo for transfusions. Platelets are formed when megakaryocytes (Mks) undergo extensive cytoskeletal rearrangements to create proplatelets (proPLTs), which are precursors to platelets [3]. Mks arise from differentiated hematopoietic stem and progenitor cells (HSPCs) as they migrate over a gradient of oxygen tension—with hypoxic conditions near the bone and higher O_2 concentrations at the vasculature [4, 5]. Mature Mks displaying CD41 and CD42b markers undergo endomitosis (polyploidization) to give rise to high-ploidy Mks [6–9]. Finally, Mks

extend proPLTs into the blood sinuses where shear forces fragment proPLTs into platelets [10]. Mks can also enter the blood and get trapped in the lung capillary bed where high shear forces process Mks into platelets [11–14].

A major challenge of generating large numbers of culture-derived platelets is producing large numbers of mature Mks from each input $CD34^+$ cell [15–17]. Mks can be derived from either umbilical cord blood, bone marrow, or mobilized peripheral blood (mPB) $CD34^+$ HSPCs [15]. Also, induced pluripotent stem cells (iPSCs) have been used to generate Mks and Mk cell lines [18–21]. Media conditions and cytokine combinations, as well as manipulating the pH and pO_2 during culture, are continuously being optimized for Mk production [22–24]. Although HSPC expansion has been studied in various technologies such as two-dimensional static cultures, stirred systems and rocking culture bags [25, 26], there has been minimal evaluation of new technologies for Mk production. Developing new culture processes for generating Mks should also improve culture productivities. Yang et al. demonstrated that a rotary cell culture system, which keeps cells in a continuous free-falling three-dimensional environment, enhanced the number of mature Mks from CB $CD34^+$ cells [27].

Recently, the G-Rex membrane system has been used to expand large numbers of T-cells, NK cells, HSPCs, and other cell lines within a scalable closed system [28–33]. The gas-permeable membrane provides efficient oxygen transfer from the incubator atmosphere to the cells. CO_2/O_2 diffusion is no longer dictated by the media height, which usually restricts media usage in standard tissue culture flasks and wells. The G-Rex allows the use of various cell densities and larger volumes of media without the need for numerous media exchanges. Although the G-Rex system has shown extensive benefits for other cell types, it has not been evaluated for the expansion and differentiation of $CD34^+$ cells into Mks.

We investigated the G-Rex system for Mk production from mPB $CD34^+$ cells using our three-phase protocol (Fig. 1A) [23]. Recent studies have shown that fed-batch media dilution schemes increase HSPC expansion [34] so we also studied media dilutions. A key parameter for G-Rex is the seeding cell-surface density. Previous studies using the megakaryoblastic K562 cell line showed that cell-surface densities between 125 and 1,000 $\times$ 10^3 cells per cm^2 yielded similar expansions, whereas a density of 62.5 $\times$ 10^3 cells per cm^2 produced little to no expansion [35]. We screened various cell-surface densities and found that a seeding density of 40 $\times$ 10^3 cells per cm^2 plus culturing the cells in G-Rex for the first 5 days, along with media dilutions, more than doubled Mk production per input $CD34^+$ cell compared with using a standard tissue culture surface (STCS) and full media exchanges. G-Rex conditions also increased the number of $CD34^+CD41^+$ cells produced by day 7 of culture. Although the mean Mk ploidy was lower in G-Rex cultures, these conditions produced equal or greater numbers of high-ploidy Mks compared with STCS cultures. G-Rex Mks displayed characteristic proPLT extensions and platelet-like-particles (PLPs) collected from G-Rex Mks showed in vitro functionality. These results demonstrate the potential of using gas-permeable surfaces and improved cell-culture techniques to increase ex vivo generation of Mks.

Materials and Methods

Unless otherwise specified, all reagents were obtained from Sigma–Aldrich (St. Louis, MO), cytokines from Peprotech (Rocky Hill, NJ), and antibodies for flow cytometry analysis from BD Biosciences (San Jose, CA). LSR II or LSR Fortessa (BD Biosciences) flow cytometers were used to collect data and analysis was done using FlowJo v.10 (FlowJo LLC, Ashland, OR). See Supporting Information Section S1 for additional methods.

Cell Culture

Previously frozen mPB $CD34^+$ cells obtained from the Fred Hutchinson Cancer Research Center (Seattle, WA) with Northwestern University Institutional Review Board approval were grown in 78% Iscove's Modified Dulbecco's Media (IMDM) (Gibco, Carlsbad, CA), 20% BIT 9500 Serum Substitute (StemCell, Vancouver, BC, Canada), 1% Glutamax (Gibco), 1 μg/ml low-density lipoproteins (Calbiochem, Whitehouse Station, NJ), 100 U/ml Pen/Strep, 100 ng/ml thrombopoietin (TPO), 100 ng/ml stem cell factor (SCF), 10 ng/ml interleukin (IL)-6, 10 ng/ml IL-11, and 2.5 ng/ml IL-3 (R&D Systems, Inc., Minneapolis, MN). Conditions were kept at 37°C, 5% CO_2, and 5% O_2 for 5 days (Panasonic incubator MCO-170 M, Wood Dale, IL). After day 5 and through rest of culture, cultures were grown in 37°C, 5% CO_2, and 20% O_2.

Culture conditions have been labeled in the format XyyZ, where X represents major culture type (C, G), yy is the seeding density in thousands per cm^2, and Z represents a modification (if relevant; R, D). R describes a G-Rex condition that has restricted oxygen transfer and D describes diluted conditions. For example, STCS controls and G-Rex conditions seeded at 11 $\times$ 10^3 cells per cm^2 are C11 and G11, respectively. Diluted conditions would then be C11D or G11D.

For STCS controls (C11), on day 0 cells were seeded at 40,000 cells per milliliter in 6-well (9.5 cm^2) plates with 0.28 ml of media per cm^2. On day 5, cells were resuspended in fresh media at a density of 250,000–450,000 cells per milliliter with 100 ng/ml TPO, 100 ng/ml SCF, 10 ng/ml IL-9, 10 ng/ml IL-11, and 10 ng/ml IL-3. On day 7, cells were resuspended in fresh media to a density of 450,000–600,000 cells per milliliter with 100 ng/ml TPO, 100 ng/ml SCF, and 6.25 mM nicotinamide.

G-Rex experiments had seeding cell-surface density of 40 $\times$ 10^3 cells per cm^2 (G40D), unless otherwise stated, in G-Rex 6-well (10 cm^2) or 24-well (2 cm^2) plates (Wilson Wolf Corp., Saint Paul, MN). Volumetric cell density was 40,000 cells per milliliter with 1 ml of media per cm^2. On day 5, the cells were removed from G-Rex and diluted with fresh media between a 1- and 1.5-fold dilution ratio based on initial volume. Cytokines (same as STCS day 5) were added for the full volume. On day 7, a dilution ratio with fresh media was used (between 0.3-fold and onefold) based on the day 5 volume. Cytokines (same as STCS day 7) were added for the full volume. For additional G-Rex cell-surface density screening experiments see Supporting Information Figures S1, S2 and Supporting Information Tables S1-S4.

A dilution control (C11D) condition was also created, seeded similarly to STCS control C11, but at days 5 and 7 treated similarly to G-Rex cells as described above.

To minimize differences in media volumes added and media heights, on days 5 and 7, G40D and C11D dilutions targeted C11 density ranges specified above. Media heights for all conditions outside of G-Rex were kept between 0.25 and 0.30 cm. We observe donor-to-donor variability, but the same media heights were used for conditions from a single donor. After day 7, all conditions were maintained at a density between 700,000 and 1 million cells per milliliter.

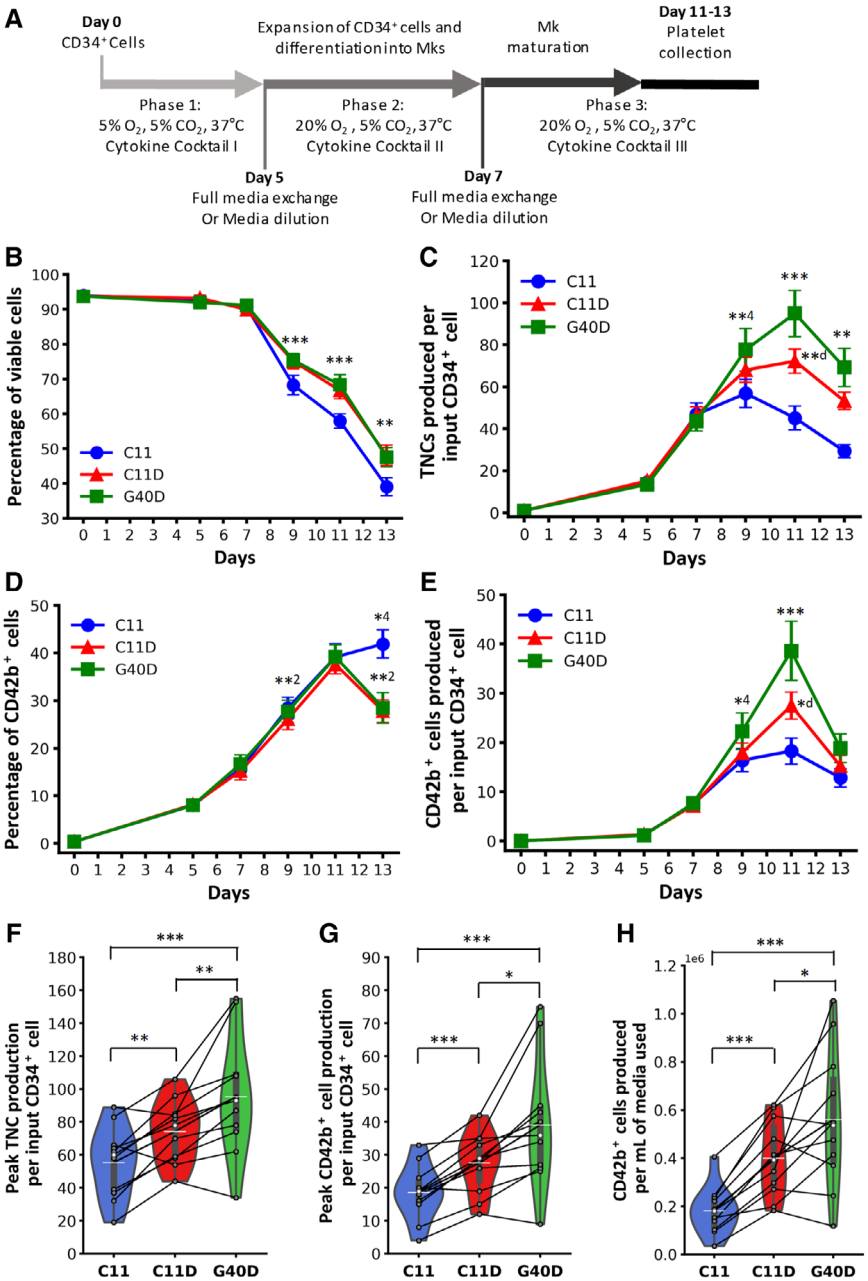

Figure 1. G-Rex and dilutions improve overall culture productivity. **(A):** Three-phase culture to expand and differentiate $CD34^+$ mobilized peripheral blood hematopoietic stem and progenitor cells into megakaryocytes, utilizing different cytokine cocktails and/or oxygen levels in each stage. **(B–E):** Time course profiles for G-Rex at seeding density of 40×10^3 cells per cm^2 with dilutions (green, G40D) compared with control (blue, C11), and dilution control (red, C11D). (B): Viability profiles. (C): Viable total nucleated cell (TNC) fold expansion per input $CD34^+$ cell. (D, E): The percentage of cells that are $CD41^+CD42b^+$ and production of $CD41^+CD42b^+$ cells per input $CD34^+$ cell over time. Points = mean ± SEM. n = 11 for all points except day 13 where n = 9. For points with both C11D and G40D significantly different from C11: ***, $p < .001$; **, $p < .01$; *, $p < .05$. For G40D versus C11 only **4, $p < .01$; *4, $p < .05$. For G40D versus C11D only **d, $p < .01$; *d, $p < .05$. For C11D versus C11 only **2, $p < .01$. Violin plots for **(F)** peak TNC production, **(G)** peak $CD42b^+$ cells produced per input $CD34^+$ cell and **(H)** $CD42b^+$ cells produced per milliliter of media used. Individual donors (n = 11) represented as gray dots and connected by lines. White dot = median, black bars = 25/75 quantiles, white line = mean.

Flow Cytometry

Cells were washed twice at 4°C with cold PEB (phosphate-buffered saline [PBS] with 2 mM EDTA and 0.5% bovine serum albumin [BSA]). Antibodies anti-CD41-FITC (555466), anti-CD42b-APC (551061), and anti-CD34-PE (555822) were added to the samples and incubated for 30 minutes at 4°C. Cells were washed twice with PEB and incubated with DAPI (Invitrogen, Carslbad, CA) for 15 minutes at room temperature before analysis.

Mk Ploidy Analysis

Cells were washed twice at 4°C with cold PEB and then incubated with anti-CD41 antibody for 30 minutes at 4°C. Cells

were washed twice with PEB and then fixed with 0.5% paraformaldehyde in PBS and incubated for 15 minutes at room temperature. Cells were then permeabilized with 70% methanol for 1 hour at 4°C, treated with RNase for 30 minutes at 37°C and finally incubated with 50 μg/ml of propidium iodide to stain DNA before analysis.

PLP Preparation and Collection

Cells from G-Rex condition in a culture dish at a cell density of 1×10^6 cells per milliliter were placed on an orbital shaker (SK-O180-E, SCILOGEX, Rocky Hill, CT) set to 50 rpm on day 11. On day 13, cells were spun out and then the supernatant spun down to pellet PLPs. Pellet was resuspended in HEPES/Tyrode's buffer (10 mM HEPES, 137 mM NaCl, 2.8 mM KCl, 1 mM $MgCl_2$, 12 mM $NaHCO_3$, 0.4 mM Na_2HPO_4, 0.35% BSA, 5.5 mM glucose, pH 7.4).

PLP Flow Cytometry

PLP suspension was analyzed with antibodies against CD41, CD42b, CD62P (564038), and PAC-1 (340507). Thrombin at 3 U/ml was added to activate PLPs and samples were incubated for 15 minutes at room temperature. Expression of markers on PLPs was compared with unactivated (no thrombin), stained samples.

Statistical Analysis

Paired *t* tests were conducted for all pairs of conditions, and the significance level was set at $p < .05$. Bar graphs and plots are shown with SEM and SD (used in Figs. 5 and 6).

RESULTS

Cell-Surface Density of 40×10^3 Cells per cm^2 in G-Rex Improves Total Nucleated Cell and Mk Production

Through early screening experiments with single donors, we identified that seeding the cells at a surface density of 40×10^3 cells per cm^2 through the first 5 days of culture and employing media dilutions on days 5 and 7 provided effective $CD42b^+$ Mk production (see Supporting Information Section S2.1 for screening data). We further investigated this condition, G40D—comparing it to a dilution control C11D and the standard process C11. The viability of G40D and C11D remained significantly higher compared with C11, which correlated with an increased viable total nucleated cell (TNC) for these conditions by day 11 (Fig. 1B, 1C). The $CD41^+$ cell fraction over time was similar across the conditions until day 13 and $CD41^+$ cell production per input $CD34^+$ cell was greatest in G40D by day 11 (Supporting Information Fig. S3A, S3B). The % $CD41^+CD42b^+$ cells increased similarly across the conditions with G40D cultures generating on average larger numbers of $CD42b^+$ cells produced per input $CD34^+$ cell by day 11 (Fig. 1D, 1E). Interestingly, there was a larger drop in purity and Mk numbers on day 13 in both C11D and G40D compared with C11.

Peak TNC expansion per input $CD34^+$ cell was significantly higher in G40D compared with all conditions, and C11D was also higher compared with C11 (C11 versus G40D, $p = 1e{-}4$; C11 versus C11D, $p = 2e{-}3$; C11D versus G40D, $p = 8e{-}3$; Fig. 1F). Peak $CD42b^+$ cell production per input $CD34^+$ cell was highest in G40D at 39 ± 19 compared with 28 ± 9 for C11D and 18 ± 8 for C11 (C11 versus G40D, $p = 3e{-}4$; C11 versus C11D, $p = 1e{-}4$; C11D versus G40D, $p = .01$; Fig. 1G). The number of $CD42b^+$ cells produced per milliliter of media used was twofold and threefold higher than C11 for C11D and G40D, respectively (C11 versus C11D, $p = 1{-}e5$; C11 versus C40D, $p = 2e{-}4$; C11D versus G40D, $p = .04$; Fig. 1H). It should be noted that there were no differences in cytokine usage between the conditions in these experiments and that G40D and C11D had similar media dilutions on days 5 and 7. Importantly, we observed positive effects for a high-performing donor that generated 29 $CD42b^+$ cells per input $CD34^+$ cell for C11 and 75 $CD42b^+$ cells for G40D and for a low-performing donor that yielded only 4 $CD42b^+$ cells for C11 but 9 $CD42b^+$ cells per input $CD34^+$ cell for G40D. Based on these results, the combination of G-Rex and media dilutions significantly improved culture productivities.

G-Rex Cells Retain CD34 Longer

CD34 expression was lost over the culture across all conditions, but surprisingly remained significantly higher in G40D (C11 versus G40D, $p = 2{-}e5$; C11D versus C40D, $p = 2e{-}4$; Fig. 2A) which produced 1.5-fold more $CD34^+$ cells by day 7 (Fig. 2B). In all conditions, we observed populations of cells that were $CD34^+CD41^+$ and $CD34^+CD41^+CD42b^+$, and G40D had consistently higher percentages of these cells (Fig. 2C–2E). On day 7, the fraction of $CD34^+CD41^+$ cells was significantly higher in G40D with nearly double the numbers of $CD34^+CD41^+$ cells produced compared with C11 and C11D (Fig. 2D). The number of $CD34^+CD41^+CD42b^+$ cells produced was also significantly higher in G40D by day 7 (Fig. 2E). G40D had the lowest $\%CD34^+CD41^+$ cells on day 7 and a lower number of $CD34^+CD41^+$ cells produced (Supporting Information Fig. S4). Since the TNC fold expansion on day 7 was similar across conditions (Fig. 1C), these results suggest that the G-Rex affected the retention of CD34. This was likely not due to the media dilution since C11 and C11D had similar results.

G-Rex Conditions Have Lower %High-Ploidy and Higher Numbers of 2N and 4N Mks

Mk ploidy was measured on day 11 (Fig. 3A, 3B). An additional late sample on day 13 for one donor showed a decrease in % high-ploidy fractions across all conditions, but no changes to the relative ploidy distributions (Supporting Information Fig. S5). G40D cultures exhibited generally lower ploidy than C11 cultures with a greater percentage of 2N Mks ($40\% \pm 6\%$ C11 versus $47\% \pm 5\%$ G40D, $p = 1e{-}3$, Fig. 3B). G40D also had significantly lower fractions of 6N + 8N, 16N, and 32N Mks (Fig. 3B). C11 had a higher mean ploidy (inset Fig. 3B) and increased %high-ploidy compared with G40D ($32\% \pm 7\%$ C11 versus $23\% \pm 5\%$ G40D, $p = 2e{-}4$, Fig. 3C). C11D demonstrated mean ploidy and %high-ploidy similar to G40D.

G40D generated 2.5-fold more 2N and 4N Mks, ~twofold more 6N + 8N Mks and similar numbers of 16N Mks compared with C11 (Supporting Information Fig. S6). C11D also increased 2N and 4N Mk numbers by ~1.7-fold but had minimal effect on 6N + 8N Mks (Supporting Information Fig. S6). Although G40D conditions had lower %high-ploidy, this was more than offset by the greater Mk expansion. By day 11, G40D generated 9 ± 3 high-ploidy Mks per input $CD34^+$ cell compared with 6 ± 2 for C11 and C11D ($p = 9e{-}5$, Fig. 3D). To estimate the overall PLP production potential, we calculated the total Mk DNA produced per input $CD34^+$ cell on day 11, which is equal to the sum of Mks produced per input $CD34^+$ cell for each ploidy fraction times their respective DNA content (i.e., 2N Mks = 1, 4N Mks = 2). G40D increased the total Mk DNA content by 1.8-fold (Fig. 3E; Supporting Information Table S5). Therefore, media dilutions (C11D) and G-Rex + media dilutions both decreased %high-

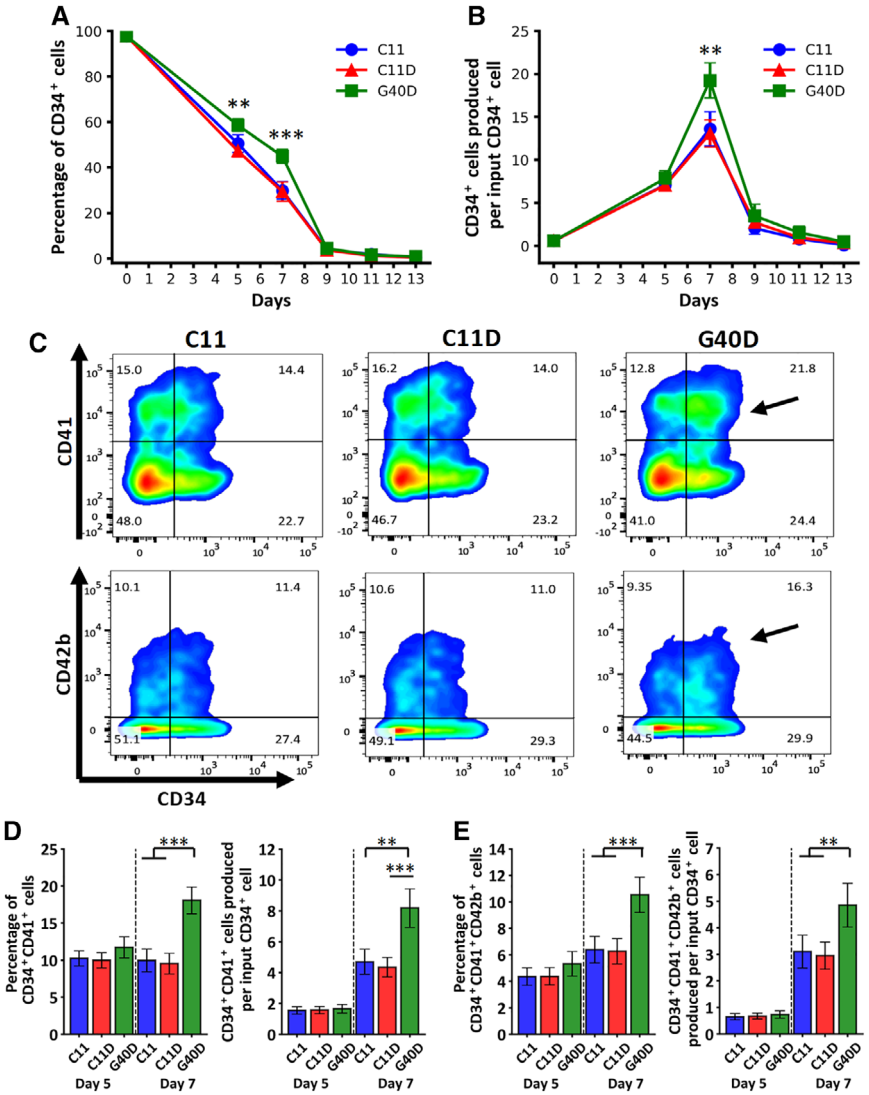

Figure 2. G-Rex cells retain CD34 longer and exhibit increased $CD34^+CD41^+$ cell production. **(A):** Percentage of the culture that is $CD34^+$ and **(B)** fold expansion of $CD34^+$ cells per input $CD34^+$ cell. **(C):** Representative flow cytometry plots on day 7 for CD41 and CD42b versus CD34 for control C11, dilution control C11D, and G40D. Black arrows denote higher percentages of $CD34^+CD41^+$ and $CD34^+CD41^+CD42b^+$ cells in G40D. For days 5 and 7, percentage and fold production of **(D)** $CD34^+CD41^+$ cells and **(E)** $CD34^+CD41^+CD42b^+$ cells. (A, B): Points = mean ± SEM, n = 11 for days 0–7, n = 9 for all other points. (D, E): Bars = mean ± SEM, n = 11. For all ***, $p < .001$; **, $p < .01$; *, $p < .05$.

ploidy, but G40D significantly expanded the Mk DNA pool compared with C11 and C11D.

G-Rex-Grown Mks Are Capable of Making proPLTs and PLPs

Next, we studied proPLT formation. Cells were seeded in wells on day 11 and proPLTs were imaged on day 13. Brightfield images of cells making proPLTs are denoted with yellow-arrow heads for C11, C11D, and G40D (Fig. 4A1, 4B1, 4C1). Additionally, confocal microscopy was used to assess proPLT morphology. Across all three conditions, polyploid cells were observed (Fig. 4A2, 4B2, 4C2). Mks undergoing initial stages of proPLT formation exhibited extensive cytoskeletal re-arragenement and thick cytoplasmic projections (Fig. 4A3, 4B3, 4C3) eventually leading to beads-on-a-string extensions (Fig. 4A4, 4B4, 4C4). We have previously shown that Mks from our standard culture process can generate PLPs after shaking the suspension on an orbital shaker [23]. To evaluate the quality of PLPs from G40D cultures, cells were shaken starting on day 11 and sampled on day 13. $CD42b^+$ PLPs demonstrated the potential for activation in the presence of thrombin via the binding of PAC-1 (Fig. 4D) and via translocation of CD62P to the membrane (Fig. 4E). Additionally, confocal analysis of the collected PLPs showed characteristic changes in morphology when thrombin was added, as they spread on fibrinogen and increased in surface area (Fig. 4F). Finally, PLPs were able to form clots within a flow aggregation study in the presence of ADP over a fibrinogen-coated surface (Fig. 4G).

Increased Mk Production Is Driven by Media Retention and an Increase in Mk Progenitors at Higher G-Rex Densities

We sought to understand what was driving the increase in Mk production from G40D conditions. First, the soft-surface was analyzed by using modified G-Rex devices that restricted oxygen transfer across the membrane (G11R) and thus operated as standard culture wells in terms of oxygen transfer. Second, the impact of improved oxygen transfer and higher oxygen tension

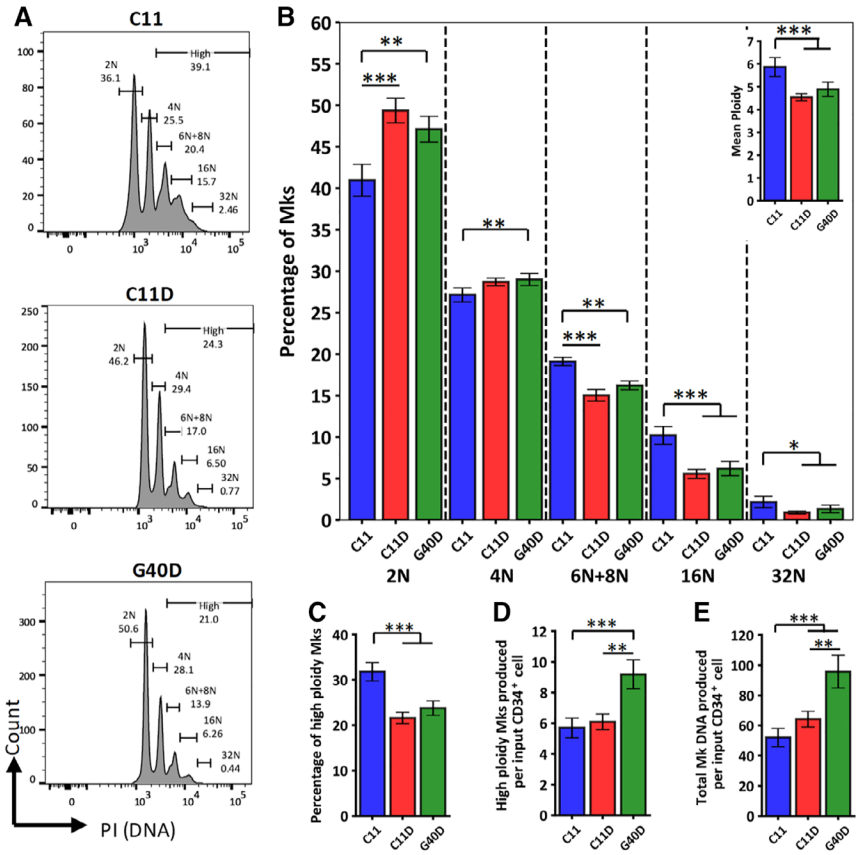

Figure 3. G-Rex with media dilutions have lower %high-ploidy but greater total megakaryocyte (Mk) DNA. **(A):** Representative day 11 ploidy plots for control C11, dilution control C11D, and G40D conditions. **(B):** The percentages of 2N, 4N, 6N + 8N, 16N, and 32N cells with inset showing mean ploidy. **(C):** %high-ploidy (>4N) of each condition. **(D):** Number of high-ploidy (>4N) Mks produced per input $CD34^+$ cell. **(E):** Total Mk DNA produced is equal to the sum of Mks produced per input $CD34^+$ cell for each ploidy fraction times their respective DNA content (i.e., 2N Mks = 1, 4N Mks = 2; see Supporting Information Table S5 for example). Bars = mean ± SEM, n = 11; ***, $p < .001$; **, $p < .01$; *, $p < .05$.

was evaluated by comparing G11R to nonrestrcited G11 cultures (standard G-Rex device). The G11R and G11 conditions were seeded at same cell-surface densities as C11. Third, standard G-Rex devices were tested across four increasing seeding densities G11, G25, G40, and G80. Finally, media dilutions were evaluated across all conditions, that is, G40 versus G40D (Fig. 5A).

TNC and Mk expansion between C11 and G11R were similar demonstrating that the soft surface at this density has minimal impact (Fig. 5B1, 5B2). However, G11 cultures had on average lower production than G11R and C11 cultures and seemed to have delayed TNC expansion, Mk commitment and Mk production (Fig. 5B1, 5B2; Supporting Information Fig. S7). This could potentially be attributed to higher oxygen tension near the cells in G11. There were no differences in $\%CD34^+CD41^+$ cells by day 7 (Fig. 5B3) and there was a greater increase in %high-ploidy Mks by day 11 for G11R and G11 compared with C11 (Fig. 5B4). For all conditions, media dilutions improved TNC and Mk expansion, while reducing %high-ploidy.

Increasing the G-Rex seeding density appeared to overcome the expansion limitation seen for G11 with further positive effects with media dilutions (Fig. 5C1, 5C2; Supporting Information Fig. S7). At surface densities above 25×10^3 cells per cm^2, the $\%CD34^+CD41^+$ cells were significantly higher by day 7 regardless of media dilutions (Fig. 5C3). Our high-surface-density screening experiments (≥100×10^3 cells per cm^2) also had higher $\%CD34^+CD41^+$ cells that further increased from day 7 to day 9 compared with controls (Supporting Information Fig. S8). G40D cells kept in G-Rex until day 7 (G40DL) had higher $\%CD34^+CD41^+$ cells (Supporting Information Fig. S9). %High-ploidy decreased with increasing surface density among diluted conditions (Fig. 5C4). For all conditions shown in Figure 5, culture viability was higher with media dilutions (Supporting Information Fig. S10).

Given that media dilutions improved expansion regardless of surface, system, or seeding density, we further explored the media component in G40D (Fig. 6A). We exchanged the media once on either day 7 (G40D-x7) or day 9 (G40D-x9) and also tested a diluted condition without any IL-3 added on day 5 (G40D-3i) since studies have shown that IL-3 could preferentially expand $CD34^+CD41^+$ Mk progenitors [36, 37]. Compared with C11, peak TNC production for G40D-x7 was comparable and for G40D-x9 it was ~1.4-fold higher (Fig. 6B). Additionally, G40D-x9 peak Mk production was ~1.6-fold higher than C11 (Fig. 6C). G40D-3i had a slower expansion (Supporting Information Fig. S11A–S11D) but peak Mk numbers were ultimately ~1.5-fold higher than C11 and ~25% lower than G40D (Fig. 6C). Compared with G40D, viability was lower and %high-ploidy was higher due to lower numbers of 2N and 4N Mks for G40D-x7, G40D-x9, and G40D-3i (Fig. 6D, 6E; Supporting Information Fig. S11E, S11F). The total Mk DNA produced per input $CD34^+$ cell for G40D-x7, G40D-x9, and G40D-3i was ~30% lower than G40D but ~1.4-fold higher than C11 (Fig. 6F). Also, $\%CD34^+CD41^+$ cell fractions remianed high in

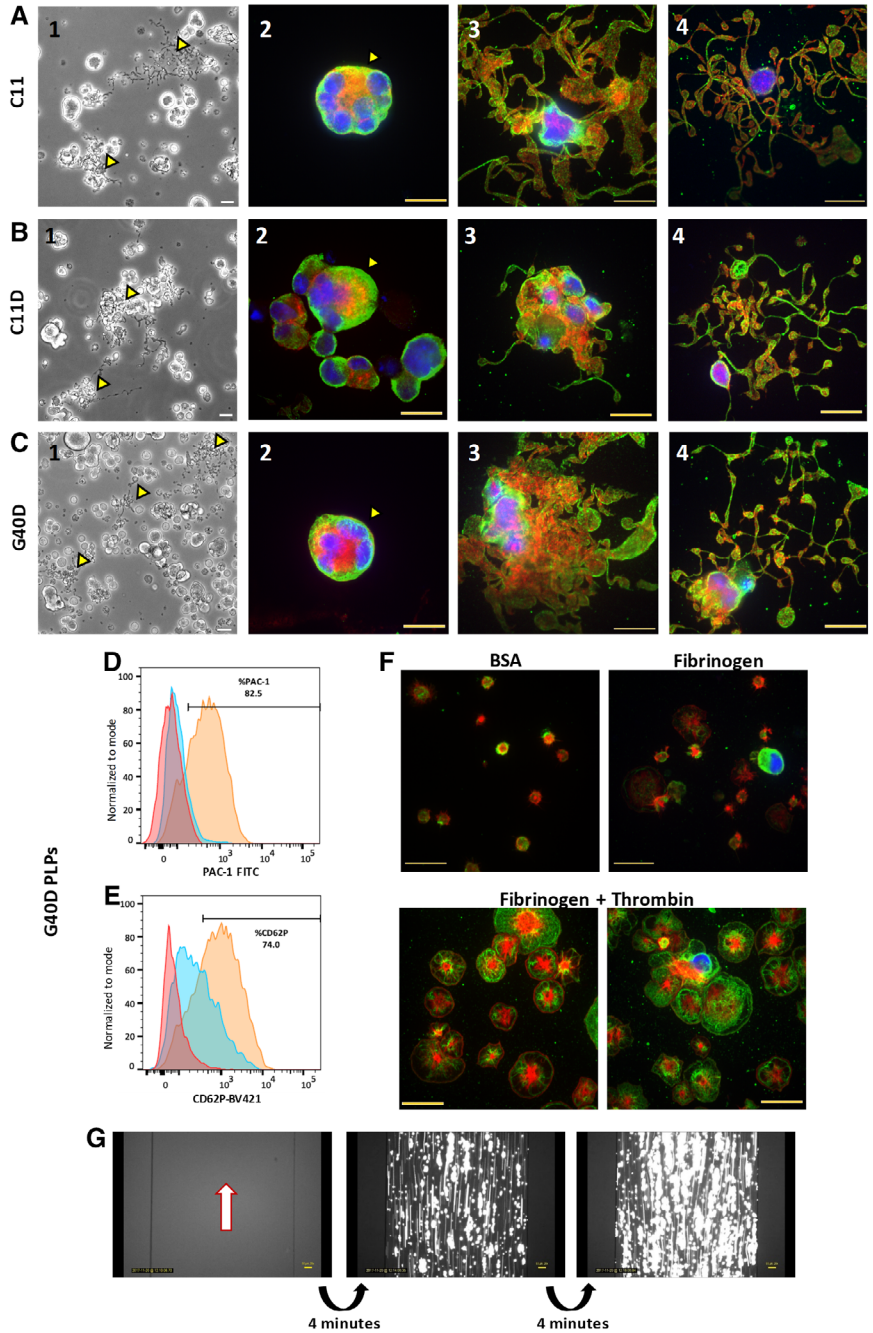

Figure 4. G-Rex Mks form proplatelets (proPLTs) and generate platelet-like-particles (PLPs). proPLT formation on day 13 for culture conditions C11 **(A)**, dilution control C11D **(B)**, and G40D **(C)**. **(1):** Brightfield images with yellow arrow-heads pointing to proPLT-making megakaryocytes (Mks). **(2):** Large high-ploidy Mk (yellow arrow-head). **(3):** Early stages of proPLT formation. **(4):** Late-stage proPLT formation. Scale bars = 15 μm. **(D):** PAC-1 binding of G40D-PLPs in the absence (blue) and presence (orange) of thrombin. **(E):** CD62P expression of G40D-PLPs in the absence (blue) and presence (orange) of thrombin. For (D) and (E), analysis shown for gated $CD42b^+$ PLPs, and the unstained sample shown as red. **(F):** Confocal microscopy analysis of resting G40D-PLPs on BSA and on fibrinogen in the absence (upper) or presence (2 lower) of thrombin. Scale bar = 15 μm. **(G):** Collected G40D-PLPs were introduced into a fibrinogen-coated flow chamber to demonstrate aggregation potential in the presence of 25 μM ADP and 2 mM $CaCl_2$. Images shown are 4 minutes apart. PLPs have been stained with Calcein AM. White arrow is direction of flow. Scale bar = 50 μm. For confocal images, red = actin, green = β-tubulin, blue = DNA.

G40D-3i compared with C11 and C11D (Fig. 6G). Overall, the results of Figures 5 and 6 demonstrate that increasing G-Rex cell-surface density improved expansion while at the same time increasing $\%CD34^+CD41^+$ cell fractions, whereas media/IL-3 retention significantly improved culture productivity.

Discussion

Various studies have demonstrated benefits of the G-Rex system for expanding different cell types due to their scalability, improved oxygen transfer, and higher culture viability [32, 38].

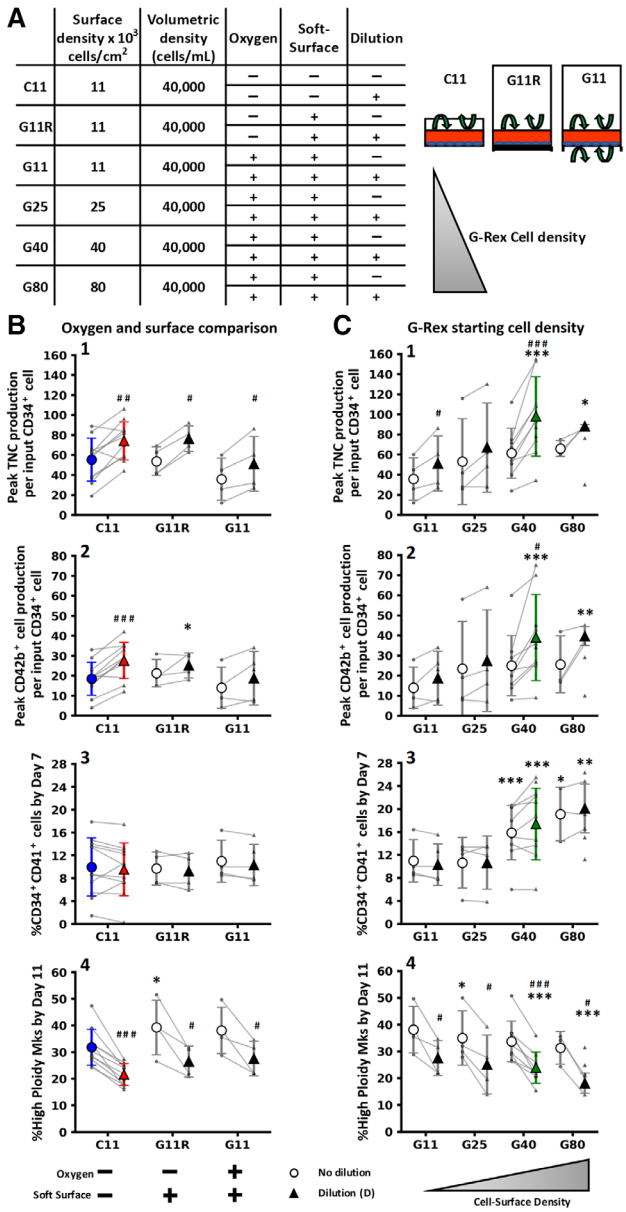

Figure 5. Factors contributing to expansion in G-Rex cultures. **(A):** Experimental layout for variables that may affect megakaryocyte (Mk) expansion. **(B):** Oxygen and surface comparison across C11, a restricted oxygen G-Rex device (G11R), and a standard G-Rex device (G11) all seeded at the same cell surface density of 11×10^3 cells per cm^2. **(C):** Increasing G-Rex cell-surface density: 11 (G11), 25 (G25), 40 (G40), and 80 (G80) $\times 10^3$ cells per cm^2. All conditions in (B) and (C) were also tested with dilution (triangle) or no dilution (open circle). Mean (±SD) calculated for conditions using paired points with gray lines connecting individual donors across diluted/nondiluted conditions. Dilution denoted with "D" added to condition name. Total cultures C11/C11D, $n = 11$; G11R/G11RD, $n = 4$; G11, $n = 4$; G11D, $n = 5$; G25/G25D, $n = 4$; G40, $n = 9$; G40D, $n = 11$; G80, $n = 3$ and G80D, $n = 6$. Statistics were evaluated by comparing **(1)** to respective C11 controls paired across the same donors, **(2)** diluted/nondiluted conditions paired across the same donors (gray lines), **(3)** dilution control C11D to G-Rex conditions paired across same the donors when $n \geq 3$, and **(4)** G-Rex conditions paired across the same donors when $n \geq 3$. For reference, colors for C11 (blue), C11D (red), and G40D (green) are the same as presented starting from Figure 1. Compared with main control C11: *, $p < .05$; **, $p < .01$; ***, $p < .001$. Comparing no dilution versus dilution (gray lines): #, $p < .05$; ##, $p < .01$; ###, $p < .001$. **(B1, C1):** Peak TNC. **C11D** versus G11R**, G11*, G11D*, G40*; **G40D** versus G11R**, G11RD*, G11**, G11D**; **G11RD** versus G11**, G11D*; **G11R** versus G11*. **(B2, C2):** Peak CD42b cells. **C11D** versus G80D*; **G40D** versus G11R*, G11RD*, G11*, G11D*; **G11RD** versus G11*. **(B3, C3):** % $CD34^+CD41^+$ cells. **C11D** versus G40***, G80*, G80D**; **G40D** versus G11R**, G11RD*, G11*, G11D**, G25*, G25D*. **(C4, C4):** % high-ploidy Mks. **C11D** versus G11R*, G11RD*, G11*, G25*, G40***, G80*; **G40D** versus G11R*, G11*, G25*; **G11RD** versus G11*, **G11R** versus G11D*. Abbreviation: TNC, total nucleated cell.

Additionally, the use of fed-batch media dilutions have proven positive for the expansion of $CD34^+$ cells from CB compared with full media exchanges [34]. In this study, we used the G-Rex system coupled with a fed-batch dilution strategy to generate Mks from mPB $CD34^+$ HSPCs and identified an efficient starting cell-surface density of 40×10^3 cells per cm^2 (G40D). This cell density is much lower than the density range of $125–500 \times 10^3$ cells per cm^2 used in G-Rex cultures of K562 cells, T-cells, and other cell types [30, 35]. G40D cultures generated 39 ± 19 $CD41^+CD42b^+$ Mks per input $CD34^+$ cell, which was higher than our current process with (C11D) or without (C11) a fed-batch strategy at 28 ± 9 and 18 ± 8, respectively. G40D cultures were also higher than recently reported mPB-Mk yield of 27 [39]. C11D and G40D had increased culture viability, improved the number of Mks produced per milliliter of media used, and had lower %high-ploidy cultures with similar production of ≥16N Mks compared with C11. However, G40D cultures had higher fractions of $CD34^+CD41^+$ cells (Mk progenitors) by midculture and yielded significantly greater numbers of 2N, 4N, and 6N + 8N Mks, while increasing the total Mk DNA pool. We observed substantial donor-to-donor variability but G40D trends held true for both high and low-performing donors.

The soft silicone rubber membrane surface in the G-Rex is very different from the polystyrene culture surface used in C11/C11D. Recent studies have shown that soft surfaces could have a positive effect on HSPC expansion [40, 41]. With the same seeding cell-surface density of C11 and restricting gas-transfer across the membrane (G11R), the G-Rex soft-surface did not improve TNC or Mk expansion. Surprisingly, a G-Rex device with restricted oxygen transfer had higher expansion than a standard G-Rex device (G11R versus G11). Due to the permeable membrane, oxygen tension would be higher near the cells in G-Rex devices than in standard wells or restricted G-Rex devices. The differences in oxygen tension could explain these results since our previous studies have shown that higher oxygen tension early in culture decreases total Mk expansion [22]. Increasing the G-Rex cell-surface density up to 80×10^3 cells per cm^2 improved expansion, consistent with past G-Rex studies showing the importance of increased cell–cell contact for growth [35].

G-Rex systems have been used to expand HSPCs from various sources using a surface density of 500×10^3 cells per cm^2 that resulted in a 13.6-fold expansion of $CD34^+$ cells after 12 days [28]. In the present study after 7 days, G40D conditions yielded a 19-fold expansion of $CD34^+$ cells and contained higher fractions of $CD34^+CD41^+$ cells compared with controls. Neither the soft surface nor improved gas transfer in the G-Rex increased Mk progenitors at low cell density. Higher G-Rex cell-surface densities led to more extensive and longer CD34 retention and increased numbers of Mk progenitors regardless of dilutions. In a previous study, culturing $CD34^+$ cells at high volumetric densities increased Mk progenitor populations [42].

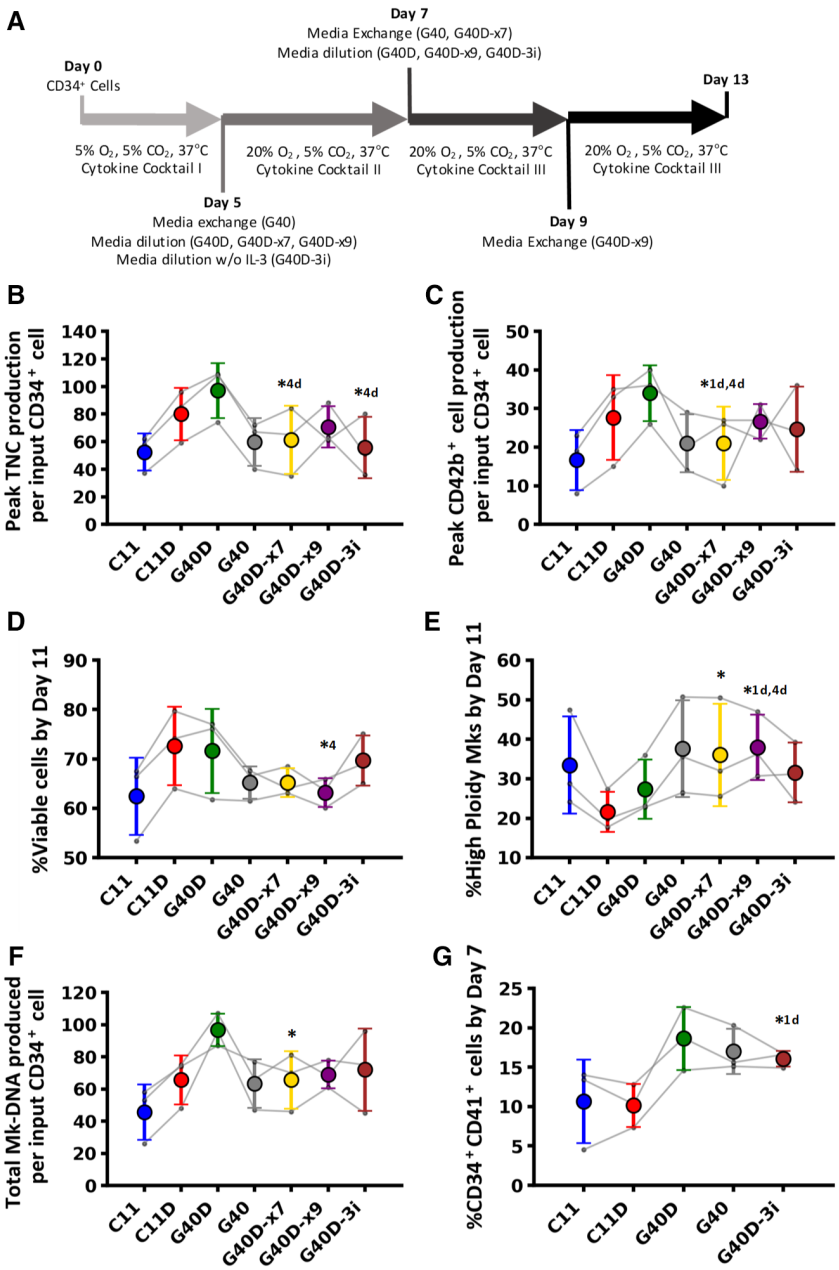

Figure 6. Late media exchange and IL-3 removal reduce megakaryocyte (Mk) expansion. **(A):** Experimental layout testing media exchanges for G-Rex cell-surface density of 40 × 10^3 cells per cm^2: no dilutions (G40), dilution days 5/7 (G40D), dilution day 5 + media exchange day 7 (G40D-x7), dilution days 5/7 + media exchange day 9 (G40D-x9), and dilution days 5/7 with no IL-3 added on day 5 (G40D-3i). Control C11 and dilution control C11D were tested as well. **(B):** Peak total nucleated cell production and **(C)** peak $CD42b^+$ cells produced per input $CD34^+$ cell. **(D):** %viable cells by day 11. **(E):** %high-ploidy Mks by day 11. **(F):** Total Mk DNA produced. **(G):** % $CD34^+CD41^+$ cells by day 7. Gray lines connect individual donors. Mean ± SD, $n = 3$; *, $p < .05$ compared with C11; *1d, $p < .05$ compared with C11D; *4, $p < .05$ compared with G40; *4d, $p < .05$ compared with G40D.

The authors seeded cells at 400,000 cells per milliliter (in 20% oxygen) and performed daily dilutions. In the present study, because a low oxygen period is used during the first 5 days of culture without disruption, cells were not seeded at higher volumetric densities in standard tissue culture wells due to concern of overgrowth and nutrient depletion along with rapid accumulation of secreted soluble factors. The use of G-Rex systems allowed us to increase seeding cell numbers while maintaining the starting volumetric density at 40,000 cells per milliliter. Importantly, volumetric and cell-surface densities after day 5 were kept similar across the conditions. Therefore, the increase in $CD34^+CD41^+$ cells is largely driven by increased cell-surface densities and cell–cell contact during the low oxygen phase in the first 5 days of culture.

Media dilutions improved productivities across all conditions. G-Rex cell-surface densities above 25 × 10^3 cells per cm^2 produced over twofold more Mks than controls. Exchanging the media on day 5, 7, or 9 diminished the expansion

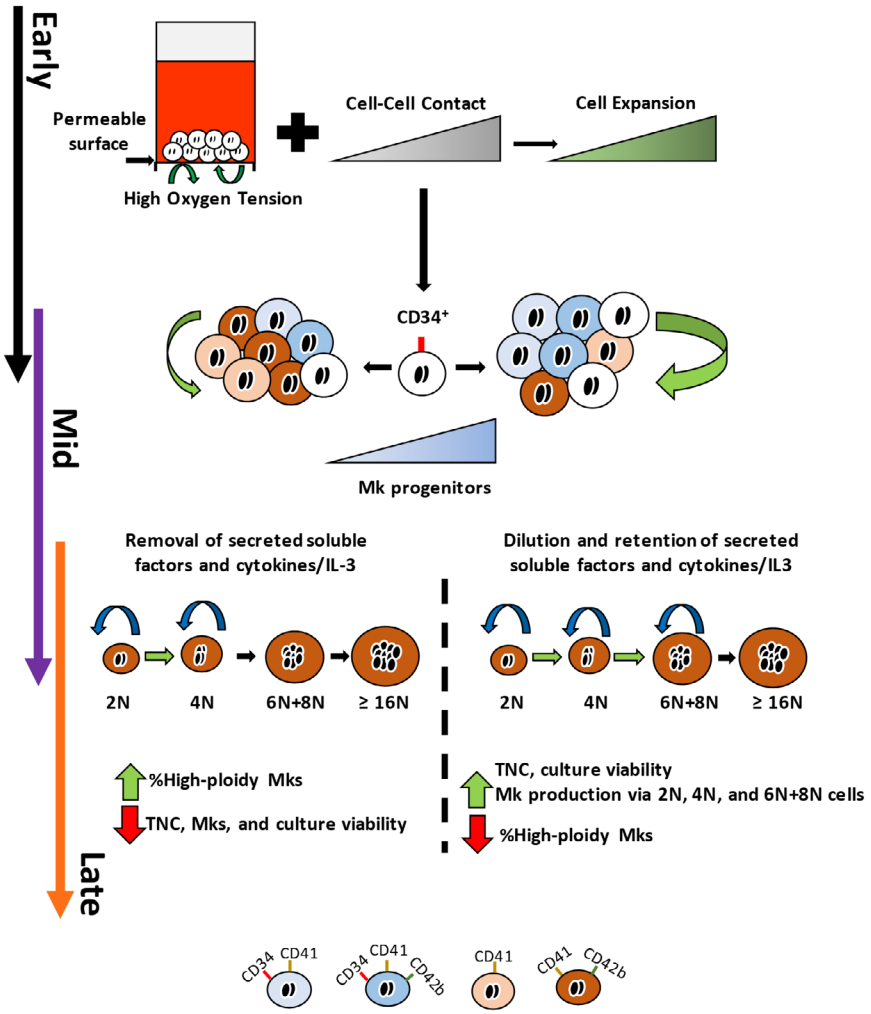

Figure 7. Proposed model of how G-Rex and media dilutions enhance megakaryocyte (Mk) production from mPB CD34$^+$ cells. High cell-surface seeding density early in G-Rex improves expansion and increases the fraction of cells that are Mk progenitors by midculture. The larger numbers of Mk progenitors benefit from retention of conditioned media and IL-3 to further expand and increase final numbers of CD41$^+$CD42b$^+$ Mks produced. Retention of the media for low G-Rex cell-surface densities or non-G-Rex devices also had a benefit on Mk expansion.

potential of G40D cultures, while reducing culture viability. It has been reported that IL-3 has a positive effect on expansion of Mk progenitors [36, 37] and our results demonstrate that retention of the conditioned media/IL-3 maintains the expansion of CD41$^+$CD42b$^+$ Mks. Although C11/C11D produced Mk progenitors, the numbers were ~twofold lower by midculture compared with G-Rex at high densities. Thus, by increasing the cell-surface density in G-Rex to produce more Mk progenitors and by retaining the conditioned media/IL-3, greater Mk numbers were produced (Fig. 7).

Ommitting IL-3 from day 5 dilutions (G40D-3i versus G40D, Fig. 6) reduced Mk production, but it was still 50% higher than C11. These observations provide evidence that the conditioned media itself retains potential for Mk production, absent fresh IL-3. It has been reported that various endogenous soluble factors are secreted by HSPCs with both a negative and positive impact on HSPC expansion [34, 43]. Positive syngergistic effects between cytokines have shown to be beneficial for Mk production, specifically between TPO, SCF, and IL-3 [23, 37]. Insulin-like growth factor-1 and insulin-like growth factor binding protein-3 secreted from Mks has been reported to support HSPC expansion [44]. Also, studies have shown that exogenous cytokines can stimulate Mks to secret IL-3 and IL-6 [45]. All these findings indicate various ways in which dilutions versus media exchange are beneficial through diluting negative factors, while retaining positive factors that benefit Mk production.

G-Rex Mks displayed proPLTs and the PLPs collected displayed in vitro activation potential and aggregation potential in flow chambers, similar to that reported for other culture-derived PLPs [46, 47]. Estimates for two different donors revealed similar levels of CD41$^+$CD42b$^+$ PLPs per input CD34$^+$ cell on day 13 between G40D, C11, and C11D (data not shown). This indicates that, although the Mk pool was expanded in G40D, we may not have changed the PLP-producing Mk population. However, we have not yet optimized PLP collection in these cultures. Microfluidic systems appear to be effective at promoting PLP release by mimicking in vivo environments [46, 48, 49]. G-Rex Mks introduced into our uniform-shear rate microbioreactor displayed similar

proPLT and PLP behavior (data not shown) as previously described for Mks cultured in STCS [48] and we are working to scale-up the bioreactor. Recent work has also identified turbulence as a key variable for PLP generation [50]. Yet, further advancements in engineering systems that can efficiently generate PLPs ex vivo are crucial [51].

Platelet transfusions typically contain 3×10^{11} platelets per unit [52]. In contrast, Mk expansion and PLP yields ex vivo remain low with required starting cell numbers approaching 10^8–10^9 input $CD34^+$ cells per unit with current methods [15, 16, 53]. The median number of $CD34^+$ cells recovered from healthy donors after G-CSF treatment was reported to be ~500 million cells [54] and with our Mk yields we could generate ~2×10^{10} Mks per donor. With a conservative yield of 15 PLPs/Mk, one donor could give rise to one platelet unit for transfusion. However, since millions of platelet units are transfused each year, to create a clinically relevant process, one donor should give rise to multiple transfusion units. Increasing our Mk yields by an order of magnitude would be a substantial improvement and lead to 10 platelet units, but would still require 10^4–10^5 donors a year.

An alternative strategy is to infuse culture-derived Mks into the body for in vivo PLP production as has been done in mice [11, 55–57]. Although the estimated yield of PLPs per infused ex vivo-derived human Mk was low (10–100) [57], G-Rex systems could be used to produce larger numbers of Mks for infusion. Additionally, transfusions of Mk progenitors have been safely reported in humans with transfusion cell numbers in the range of 10^5–10^6 Mk progenitors per kilogram of body weight [58–61]. Mk progenitors have been reported to be responsible for platelet recovery after transplantation [62, 63]. In this study, we estimate a yield of 8 ± 4 Mk progenitors produced per input $CD34^+$ cell and thus could generate 4×10^9 Mk progenitors by day 7 per donor. With a body weight of 70 kg, a single donor could provide 50–500 transfusions. Furthermore, mouse studies on the in vivo PLP potential of G-Rex-derived Mks as well as the clonogenic potential from G-Rex-derived Mk progenitors are required. Additional safety studies should address the concern of larger cell-size of Mks that could obstruct small vessels along with the concern of tumorigenesis [64]. Studies have shown, however, that irradiated iPSC-derived Mks retained potential to produce PLPs in vivo after being infused into mice [65].

Conclusion

Additional advances are clearly required to produce clinically relevant Mk numbers from the process described in this study. Future G-Rex studies would include re-examining higher seeding cell-surface densities with the fed-batch dilution method from this study, adjusting cytokine concentrations and evaluating CB HSPCs. Lower oxygen setting for the first 5 days should be explored when using G-Rex. Also, the cell–cell contact mechanism for prolonged CD34 expression could be explored. Nonetheless, our results highlight distinct methods of increasing Mk numbers through a fed-batch dilution scheme and utilizing technologies that permit higher input cell numbers.

Acknowledgments

This research was supported by NIH 1R01HL130760-01. A.F.M. was also partially supported by NIH T32 GM008449 (Predoctoral Biotechnology Training Grant). This work used Northwestern University Micro/Nano Fabrication Facility (NUFAB), partially supported by NSF ECCS-1542205 (Soft and Hybrid Nanotechnology Experimental (SHyNE) Resource), DMR-1720139 (Materials Research Science and Engineering Center), the State of Illinois, and Northwestern University. This work used the Flow Cytometry Core Facility supported by NCI CA060553 (Cancer Center Support Grant) and the Biological Imaging Facility at Northwestern University. We thank Damien Doser, Darryl Abbot, Vasil Kukushliev, and Jia Wu for helping with some of the data collection. We also thank Jia Wu for discussions on statistics and data analysis. G-Rex plates were generously supplied by Wilson Wolf.

Author Contributions

A.F.M.: conception and design, collection and assembly of data, data analysis and interpretation, manuscript writing, final approval of manuscript; W.M.M.: conception and design, data interpretation, manuscript writing, final approval of manuscript.

Disclosure of Potential Conflicts of Interest

G-Rex 6- and 24-well plates were generously provided by Wilson Wolf Corporation. Wilson Wolf did not influence the experimental design and did not provide input on the article. The authors indicated no potential conflicts of interest.

Data Availability Statement

The data that support the findings of this study are available from the corresponding author upon reasonable request.

References

1 Baigger A, Blasczyk R, Figueiredo C. Towards the manufacture of megakaryocytes and platelets for clinical application. Transfus Med Hemother 2017;44:165–173.

2 Ellingson KD, Sapiano MR, Haass KA et al. Continued decline in blood collection and transfusion in the United States—2015. Transfusion 2017;57:1588–1598.

3 Patel SR, Hartwig JH, Italiano JE. The biogenesis of platelets from megakaryocyte proplatelets. J Clin Invest 2005;115:3348–3354.

4 Chow DC, Wenning LA, Miller WM et al. Modeling pO2 distributions in the bone marrow hematopoietic compartment. II. Modified Kroghian models. Biophys J 2001;81:685–696.

5 Jež M, Rožman P, Ivanović Z et al. Concise review: The role of oxygen in hematopoietic stem cell physiology. J Cell Physiol 2015; 230:1999–2005.

6 Lordier L, Jalil A, Aurade F et al. Megakaryocyte endomitosis is a failure of late cytokinesis related to defects in the contractile ring and Rho/Rock signaling. Blood 2008; 112:3164–3174.

7 Mattia G, Vulcano F, Milazzo L et al. Different ploidy levels of megakaryocytes generated from peripheral or cord blood CD34+ cells are correlated with different levels of platelet release. Blood 2002;99: 888–897.

8 Mazzi S, Lordier L, Debili N et al. Megakaryocyte and polyploidization. Exp Hematol 2018;57:1–13.

9 Tomer A. Human marrow megakaryocyte differentiation: Multiparameter correlative analysis identifies von Willebrand factor as a sensitive and distinctive marker for early

(2N and 4N) megakaryocytes. Blood 2004; 104:2722–2727.

10 Junt T, Schulze H, Chen Z et al. Dynamic visualization of thrombopoiesis within bone marrow. Science 2007;317:1767–1770.

11 Fuentes R, Wang Y, Hirsch J et al. Infusion of mature megakaryocytes into mice yields functional platelets. J Clin Invest 2010; 120:3917–3922.

12 Kaufman RM, Airo R, Pollack S et al. Circulating megakaryocytes and platelet release in the lung. Blood 1965;26:720–731.

13 Lefrançais E, Ortiz-Muñoz G, Caudrillier A et al. The lung is a site of platelet biogenesis and a reservoir for haematopoietic progenitors. Nature 2017;544:105–109.

14 Levine R, Eldor A, Shoff P et al. Circulating megakaryocytes: Delivery of large numbers of intact, mature megakaryocytes to the lungs. Eur J Haematol 1993;51: 233–246.

15 Avanzi MP, Mitchell WB. Ex vivo production of platelets from stem cells. Br J Haematol 2014;165:237–247.

16 Lambert MP, Sullivan SK, Fuentes R et al. Challenges and promises for the development of donor-independent platelet transfusions. Blood 2013;121:3319–3324.

17 Reems J-A, Pineault N, Sun S. In vitro megakaryocyte production and platelet biogenesis: State of the art. Transfus Med Rev 2010;24:33–43.

18 Borst S, Sim X, Poncz M et al. Induced pluripotent stem cell-derived megakaryocytes and platelets for disease modeling and future clinical applications. Atertio Thromb Vasc Biol 2017;37:2007–2013.

19 Moreau T, Evans AL, Vasquez L et al. Large-scale production of megakaryocytes from human pluripotent stem cells by chemically defined forward programming. Nat Commun 2016;7:11208.

20 Nakamura S, Takayama N, Hirata S et al. Expandable megakaryocyte cell lines enable clinically applicable generation of platelets from human induced pluripotent stem cells. Cell Stem Cell 2014;14:535–548.

21 Sugimoto N, Eto K. Platelet production from induced pluripotent stem cells. J Thromb Haemost 2017;15:1717–1727.

22 Mostafa SS, Miller WM, Papoutsakis ET. Oxygen tension influences the differentiation, maturation and apoptosis of human megakaryocytes. Br J Haematol 2000;111:879–889.

23 Panuganti S, Schlinker AC, Lindholm PF et al. Three-stage ex vivo expansion of high-ploidy megakaryocytic cells: Toward large-scale platelet production. Tissue Eng Part A 2013;19: 998–1014.

24 Yang H, Miller W, Papoutsakis E. Higher pH promotes megakaryocytic maturation and apoptosis. Stem Cells 2002;20:320–328.

25 Cabrita GJ, Ferreira BS, Da Silva CL et al. Hematopoietic stem cells: From the bone to the bioreactor. Trends Biotechnol 2003;21:233–240.

26 Rodrigues CA, Fernandes TG, Diogo MM et al. Stem cell cultivation in bioreactors. Biotechnol Adv 2011;29:815–829.

27 Yang Y, Liu C, Lei X et al. Integrated biophysical and biochemical signals augment megakaryopoiesis and thrombopoiesis in a three-dimensional rotary culture system. Stem Cells Translational Medicine 2016;5:175–185.

28 Bird GA, Polsky A, Estes P et al. Expansion of human and murine hematopoietic stem and progenitor cells ex vivo without genetic modification using MYC and Bcl-2 fusion proteins. PLoS One 2014;9:e105525.

29 Dave H, Luo M, Blaney J et al. Toward a rapid production of multivirus-specific T cells targeting BKV, adenovirus, CMV, and EBV from umbilical cord blood. Mol Ther Methods Clin Dev 2017;5:13–21.

30 Forget M-A, Haymaker C, Dennison JB et al. The beneficial effects of a gas-permeable flask for expansion of tumor-infiltrating lymphocytes as reflected in their mitochondrial function and respiration capacity. Oncoimmunology 2016;5:e1057386.

31 Lapteva N, Durett AG, Sun J et al. Large-scale ex vivo expansion and characterization of natural killer cells for clinical applications. Cytotherapy 2012;14:1131–1143.

32 Vera JF, Brenner LJ, Gerdemann U et al. Accelerated production of antigen-specific T-cells for pre-clinical and clinical applications using Gas-permeable Rapid Expansion cultureware (G-Rex). J Immunother 2010; 33:305–315.

33 Gerdemann U, Katari UL, Papadopoulou A et al. Safety and clinical efficacy of rapidly-generated trivirus-directed T cells as treatment for adenovirus, EBV, and CMV infections after allogeneic hematopoietic stem cell transplant. Mol Ther 2013;21:2113–2121.

34 Csaszar E, Kirouac DC, Yu M et al. Rapid expansion of human hematopoietic stem cells by automated control of inhibitory feedback signaling. Cell Stem Cell 2012;10:218–229.

35 Bajgain P, Mucharla R, Wilson J et al. Optimizing the production of suspension cells using the G-Rex "M" series. Mol Ther Methods Clin Dev 2014;1:14015.

36 Debili N, Hegyi E, Navarro S et al. In vitro effects of hematopoietic growth factors on the proliferation, endoreplication, and maturation of human megakaryocytes. Blood 1991; 77:2326–2338.

37 Broudy VC, Lin N, Kaushansky K. Thrombopoietin (c-mpl ligand) acts synergistically with erythropoietin, stem cell factor, and interleukin-11 to enhance murine megakaryocyte colony growth and increases megakaryocyte ploidy in vitro. Blood 1995; 85:1719–1726.

38 Wang X, Rivière I. Manufacture of tumor-and virus-specific T lymphocytes for adoptive cell therapies. Cancer Gene Ther 2015;22:85–94.

39 Ivetic N, Nazi I, Karim N et al. Producing megakaryocytes from a human peripheral blood source. Transfusion 2016;56:1066–1074.

40 Choi JS, Mahadik BP, Harley BA. Engineering the hematopoietic stem cell niche: Frontiers in biomaterial science. Biotechnol J 2015;10:1529–1545.

41 Holst J, Watson S, Lord MS et al. Substrate elasticity provides mechanical signals for the expansion of hemopoietic stem and progenitor cells. Nat Biotechnol 2010;28: 1123–1128.

42 Lefebvre P, Winter JN, Meng Y et al. Ex vivo expansion of early and late megakaryocyte progenitors. J Hematother Stem Cell Res 2000;9:913–921.

43 Majka M, Janowska-Wieczorek A, Ratajczak J et al. Numerous growth factors, cytokines, and chemokines are secreted by human CD34+ cells, myeloblasts, erythroblasts, and megakaryoblasts and regulate normal hematopoiesis in an autocrine/paracrine manner. Blood 2001;97:3075–3085.

44 Heazlewood SY, Neaves RJ, Williams B et al. Megakaryocytes co-localise with hemopoietic stem cells and release cytokines that up-regulate stem cell proliferation. Stem Cell Res 2013;11:782–792.

45 Wickenhauser C, Lorenzen J, Thiele J et al. Secretion of cytokines (interleukins-1 alpha,-3, and-6 and granulocyte-macrophage colony-stimulating factor) by normal human bone marrow megakaryocytes. Blood 1995; 85:685–691.

46 Blin A, Le Goff A, Magniez A et al. Microfluidic model of the platelet-generating organ: Beyond bone marrow biomimetics. Sci Rep 2016;6:21700.

47 Di Buduo CA, Wray LS, Tozzi L et al. Programmable 3D silk bone marrow niche for platelet generation ex vivo and modeling of megakaryopoiesis pathologies. Blood 2015;125: 2254–2264.

48 Martinez AF, Mcmahon RD, Horner M et al. A uniform-shear rate microfluidic bioreactor for real-time study of proplatelet formation and rapidly-released platelets. Biotechnol Prog 2017;33:1614–1629.

49 Thon JN, Mazutis L, Wu S et al. Platelet bioreactor-on-a-chip. Blood 2014;124:1857–1867.

50 Ito Y, Nakamura S, Sugimoto N et al. Turbulence activates platelet biogenesis to enable clinical scale ex vivo production. Cell 2018;174:636–648. e618.

51 Thon JN, Dykstra BJ, Beaulieu LM. Platelet bioreactor: Accelerated evolution of design and manufacture. Platelets 2017;28:472–477.

52 Cid J, Lozano M. Platelet dose for prophylactic platelet transfusions. Expert Rev Hematol 2010;3:397–400.

53 An HH, Poncz M, Chou ST. Induced pluripotent stem cell-derived red blood cells, megakaryocytes, and platelets: Progress and challenges. Curr Stem Cell Rep 2018;4:310–317.

54 Hölig K. G-CSF in healthy allogeneic stem cell donors. Transfus Med Hemother 2013;40:225–235.

55 Jarocha D, Vo KK, Lyde RB et al. Enhancing functional platelet release in vivo from in vitro—Grown megakaryocytes using small molecule inhibitors. Blood Adv 2018;2:597–606.

56 Wang H, Ge W, Zhuang Y et al. Fast recovery of platelet production in NOD/SCID mice after transplantation with ex vivo expansion of megakaryocyte from cord blood CD34+ cells. J Cancer Res Ther 2018;14:233–239.

57 Wang Y, Hayes V, Jarocha D et al. Comparative analysis of human ex vivo-generated platelets vs megakaryocyte-generated platelets in mice: A cautionary tale. Blood 2015;125: 3627–3636.

58 Decaudin D, Vantelon J, Bourhis J et al. Ex vivo expansion of megakaryocyte precursor cells in autologous stem cell transplantation for relapsed malignant lymphoma. Bone Marrow Transplant 2004;34:1089–1093.

59 Xi J, Zhu H, Liu D et al. Infusion of megakaryocytic progenitor products generated from cord blood hematopoietic stem/progenitor cells:

Results of the phase 1 study. PLoS One 2013;8: e54941.

60 Scheding S, Bergmannn M, Rathke G et al. Additional transplantation of ex vivo generated megakaryocytic cells after high-dose chemotherapy. Haematologica 2004;89: 630–631.

61 Bertolini F, Battaglia M, Pedrazzoli P et al. Megakaryocytic progenitors can be generated ex vivo and safely administered to autologous peripheral blood progenitor cell transplant recipients. Blood 1997;89:2679–2688.

62 Bruyn CD, Delforge A, Martiat P et al. Ex vivo expansion of megakaryocyte progenitor cells: Cord blood versus mobilized peripheral blood. Stem Cells Dev 2005;14:415–424.

63 Begemann P, Hassan H, Kröger N et al. Correlation of time to platelet engraftment with amount of transplanted CD34+ CD41+ cells after allogeneic bone marrow transplantation. J Hematother Stem Cell Res 2002;11:321–326.

64 Gollomp K, Lambert MP, Poncz M. Current status of blood 'pharming': Megakaryoctye transfusions as a source of platelets. Curr Opin Hematol 2017;24:565–571.

65 Eicke D, Baigger A, Schulze K et al. Large-scale production of megakaryocytes in microcarrier-supported stirred suspension bioreactors. Sci Rep 2018;8:10146.

See www.StemCellsTM.com for supporting information available online.